

The Eurasia Proceedings of Science, Technology, Engineering and Mathematics (EPSTEM), 2025

Volume 37, Pages 629-642

**ICEAT 2025: International Conference on Engineering and Advanced Technology**

## **Lead Removal from Water Using CTAB-Enhanced Nanosilica-Coated Sand Barrier Under Continuous Flow: Experimental Study and Breakthrough Curve Modelling**

**Hanan Khalaf**

Al-Furat Al-Awsat Technical University

**Thulfikar Al-Husseini**

Al-Qadisiyah University

**Entissar Hussain**

Al-Qadisiyah University

**Abstract:** This study presents the development of a novel permeable reactive barrier (PRB) material for lead removal from contaminated water using nanosilica-coated sand enhanced with cetyltrimethylammonium bromide (CTAB). The synthesis process involves coating quartz sand with nanosilica particles in the presence of CTAB to improve the dispersion and binding of the nanoparticles. Continuous fixed-bed column experiments were conducted for up to 27 days to evaluate the performance of the modified media under different flow rates (5 and 15 milliliters per minute) with an initial lead concentration of 50 milligrams per liter. The breakthrough curves obtained were analyzed using several empirical models, including Bohart-Adams, Thomas-BDST, Belter-Cussler-Hu, Clark, and Yan models. The experimental data showed a strong agreement to the Thomas-BDST and Clark models, indicating pseudo-second-order kinetics and multilayer adsorption mechanisms. The coated media demonstrated stable hydraulic conductivity of approximately  $2.5 \times 10^{-2}$  centimeters per second throughout the operation, maintaining adequate permeability for continuous flow conditions. The findings suggest that the CTAB-enhanced nanosilica-coated sand represents a promising, cost-effective, and scalable solution for the in-situ remediation of lead-contaminated groundwater through PRB technology.

**Keywords:** Sand, Nano silica, Lead, Permeable reactive barrier, Groundwater

### **Introduction**

Heavy metal contamination, particularly by lead ( $Pb^{2+}$ ), poses a persistent threat to groundwater quality due to its high toxicity, bioaccumulative nature, and long-term environmental persistence. Lead exposure is associated with severe neurological and developmental disorders, making its removal from water sources a pressing global environmental and public health concern (Salami et al., 2022). Traditional groundwater remediation techniques such as pump-and-treat systems have demonstrated limited effectiveness in heterogeneous subsurface environments. These methods often suffer from slow contaminant extraction rates, high operational costs, and lack of sustainability (Zhao et al., 2022). As a result, in-situ treatment approaches—particularly Permeable Reactive Barriers (PRBs) have garnered increased interest. PRBs utilize reactive media to passively and continuously remove contaminants as groundwater flows through the barrier.

Among the reactive media explored for PRBs, modified sands and nanomaterials have attracted considerable attention due to their high surface area and strong sorption capacities. Nanosilica is a particularly promising

- This is an Open Access article distributed under the terms of the Creative Commons Attribution-Noncommercial 4.0 Unported License, permitting all non-commercial use, distribution, and reproduction in any medium, provided the original work is properly cited.

- Selection and peer-review under responsibility of the Organizing Committee of the Conference

candidate owing to its abundant silanol groups, chemical stability, and large specific surface area, which facilitate efficient metal ion adsorption (Nguyen Xuan Huan et al., 2018). However, one of the primary challenges in applying nanosilica in porous media is particle agglomeration and poor dispersion, which can limit performance.

To overcome these limitations, surfactants such as cetyltrimethylammonium bromide (CTAB) have been employed to improve the uniformity, adhesion, and stability of nanosilica coatings. Surfactant modification enhances the contact between nanomaterials and target ions, minimizes aggregation, and improves compatibility with porous substrates (Wang et al., 2024).

Recent studies have emphasized the potential of nanotechnology-based media for groundwater remediation. For example, (Liu et al., 2022) provided a comprehensive overview of nanomaterial applications in water sustainability, while (Deshmukh & Pathan, 2025) highlighted opportunities and challenges in deploying functionalized nanoparticles in environmental cleanup. Similarly, (Masood & Abd Ali, 2020) demonstrated that CTAB-modified media significantly improved heavy metal adsorption in simulated PRB conditions.

Building on these foundations, the present study develops a novel PRB material by coating quartz sand with nanosilica in the presence of CTAB. The objective is to enhance lead removal efficiency under continuous flow conditions. The coated media are tested using fixed-bed column experiments, and breakthrough behavior is analyzed using multiple modeling approaches to evaluate the potential of the proposed material for field-scale groundwater treatment.

## Method

### Materials

Quartz sand was obtained from the local market, washed with distilled water to remove surface impurities, oven-dried, and sieved to retain particles within the 0.6–1 mm range. The sand exhibited a porosity of 0.43, specific gravity of 1.352, hydraulic conductivity of 0.16 cm/s, and a pH of 6.81. Commercial nanosilica powder ( $\text{SiO}_2$ ) was used, with a purity of 99%, average particle size (APS) between 20–30 nm, specific surface area (SSA) ranging from 180 to 600  $\text{m}^2/\text{g}$ , bulk density below 0.1  $\text{g}/\text{cm}^3$ , and true density of 2.4  $\text{g}/\text{cm}^3$ . Lead nitrate [ $\text{Pb}(\text{NO}_3)_2$ ] supplied by BDH (England) was used to prepare synthetic lead-contaminated water. A stock solution of 1000 mg/L was prepared and diluted to achieve an influent concentration of 50 mg/L for all experiments.

### Preparation of Nanosilica-Coated Sand

The coating procedure involved dispersing CTAB (cetyltrimethylammonium bromide) in 50 mL of distilled water, with CTAB mass equal to half the mass of nanosilica (Fang, G., & Fang, 2012) followed by pH adjustment to 10 using HCl. Nanosilica was added at a ratio of 0.5% (w/w) relative to the sand mass, and the mixture was stirred at 250 rpm for 6 hours to ensure homogeneous dispersion. Afterward, 100 g of dried quartz sand was introduced into the suspension and stirred for an additional 6 hours. The coated sand was dried in an oven at 105°C to promote nanoparticle adhesion, rinsed repeatedly with distilled water until the effluent pH stabilized between 7–8, then oven-dried again at 105°C for 24 hours and stored for subsequent use.

### Continuous Experiments

Column tests were conducted to evaluate the performance of the coated media under dynamic conditions. The setup included a PVC column (2.5 cm inner diameter, 50 cm height) packed with the coated sand to a depth of 50 cm. A Submersible pump delivered the influent solution from the bottom to the top at controlled flow rates of 5 mL/min and 15 mL/min. Effluent samples were collected at intervals and filtered prior to lead concentration analysis using Atomic Absorption Spectroscopy (AAS). The system was operated under laminar flow conditions ( $\text{Re} < 10$ ) to mimic natural subsurface conditions. Hydraulic conductivity (K) was determined using Darcy's law:

$$K = QA/i \quad (1)$$

Where:

- K is the hydraulic conductivity (cm/s),

- $Q$  is the volumetric flow rate ( $\text{cm}^3/\text{s}$ ),
- $A$  is the cross-sectional area of the column ( $\text{cm}^2$ ),
- $i$  is the hydraulic gradient (dimensionless).



Figure 1. Column setup elements arranged for continuous operation.

### Description of Breakthrough Curves Data

The efficacy of the fixed bed column has been forecasted utilising mathematical breakthrough curve models, which have also been employed to determine kinetic constants and uptake capacities. The breakthrough curves may be modelled using the subsequent frameworks:

#### *Adams-Bohart Model*

Adams and Bohart developed a necessary equation defining the link between  $C_e/C_o$  and time. The derivation was predicated on the idea that the concentration of the sorbate and the residual capacity of the sorbent determine the sorption rate in turn(Radhika et al., 2018). This model is appropriate for characterising the first segment of the breakthrough curve; so, it suggests that sorption is not immediate and that the sorbate concentration and residual sorption capacity of the sorbent determine the sorption rate. This model's framework looks like this(Yaqubi et al., 2021):

$$C_e/C_o = 1/(1 + \exp(KN_o \frac{Z}{U} - Kc_o t)) \quad (2)$$

Calculated by dividing the flow rate ( $\text{cm}^3/\text{min}$ ) by the cross-sectional area of the column,  $U$  is the linear velocity ( $\text{cm}/\text{min}$ ),  $K$  represents the kinetic constant ( $\text{L}/\text{g} \cdot \text{min}$ ),  $N_o$  denotes the solute concentration at saturation ( $\text{mg}/\text{L}$ ),  $Z$  indicates the bed depth ( $\text{cm}$ ),  $t$  marks the elapsed time ( $\text{min}$ ). The constants  $K$  and  $N_o$  of the Adams-Bohart model can be approximated by nonlinear regression.

#### *Thomas-BDST Model*

The bed-depth-service-time (BDST) model, sometimes referred to as the Thomas model, assesses the performance of fixed-bed columns. It forecasts the sorbent's maximal solute absorption and delineates the progression of the breakthrough curve (de Franco et al., 2017). The model presumes minimal axial dispersion and utilises a Langmuir

isotherm alongside pseudo-second-order kinetics to characterise sorption (Yaqubi et al., 2021). The Thomas model provides a precise representation of the entire breakthrough, unlike the Adams–Bohart approach profile(Nguyen et al., 2015). This document presents a mathematical characterisation of the model.

$$\frac{c}{c_o} = 1/1 + \exp ((K_T/Q) qM - K_T c_o t) \quad (3)$$

M is the mass of sorbent in the column (g); Q is the volumetric flow rate (mL/min); q is the maximum sorption capacity (mg/g) of the solid particles; and K<sub>T</sub> marks the Thomas rate constant (mL/mg.min).

#### *Yan Model*

The Yan model, or modified dose-response model, was introduced to mitigate the inaccuracies associated with the Thomas model, especially during extremely short and lengthy operational durations(de Franco et al., 2017). The Yan model was created since the earlier Thomas model cannot accommodate a fixed effluent sorbate concentration at time zero, which may restrict the simulation (Ye et al., 2020). The Yan model can be expressed using the following formula:

$$\frac{c}{c_o} = 1 - 1/1 + ((0.001 * Q * c/q_o * M) * t)^a \quad (4)$$

#### *Belter-Cussler-Hu Model*

This model is calibrated using the groundbreaking data gathered by (Chu et al., 2011). The breakthrough results indicate that this semi-empirical formula outperformed the Bohart-Adams equation; consequently, the breakthrough curves for fixed beds in the packed column are delineated as follows:

$$\frac{c}{c_o} = 1 + \text{erf} [(t - t_o) \exp(-\sigma(t/t_o)) / \sqrt{2}\sigma t_o] \quad (5)$$

where  $\sigma$  represents the standard deviation indicating the slope of the breakthrough curve, and  $t_o$  is the duration (in minutes) that must correspond to 50% of C/Co.

#### *Clark Model*

Clark (1987) developed a simulation for breakthrough curves applicable to column adsorption. The Freundlich isotherm and the mass-transfer concept were employed in this model to illustrate the relationship for the breakthrough curve as follows (Madan et al., 2019):

$$(\frac{c}{c_o})^{n-1} = 1/1 + A \cdot e^{-rt} \quad (6)$$

where n is the exponent of the Freundlich model, and r and A are constants derived from the kinetic equation.

## Results and Discussion

### Characterization of Coated Sand

The FESEM, FTIR, and XRD results included in this section are derived from a previous, unpublished study conducted by the authors using the same coated sand material prepared under identical conditions. These figures are provided here to support the structural and chemical characterization of the nanosilica-coated sand with CTAB modification.

X-ray diffraction (XRD) analysis was conducted to assess the mineralogical structure of both raw and coated sand. As shown in Figure 2, the uncoated sand exhibited characteristic peaks corresponding to quartz and minor metal oxides (e.g., CuO, SiO<sub>2</sub>), consistent with ICDD standards. Upon coating, additional diffraction peaks appeared at multiple 2θ positions (e.g., 20.9°, 26.7°, 36.6°, etc.), indicating structural modifications and the formation of new active sites. These changes suggest enhanced surface reactivity, potentially contributing to the improved Pb<sup>2+</sup> adsorption capacity of the coated material.

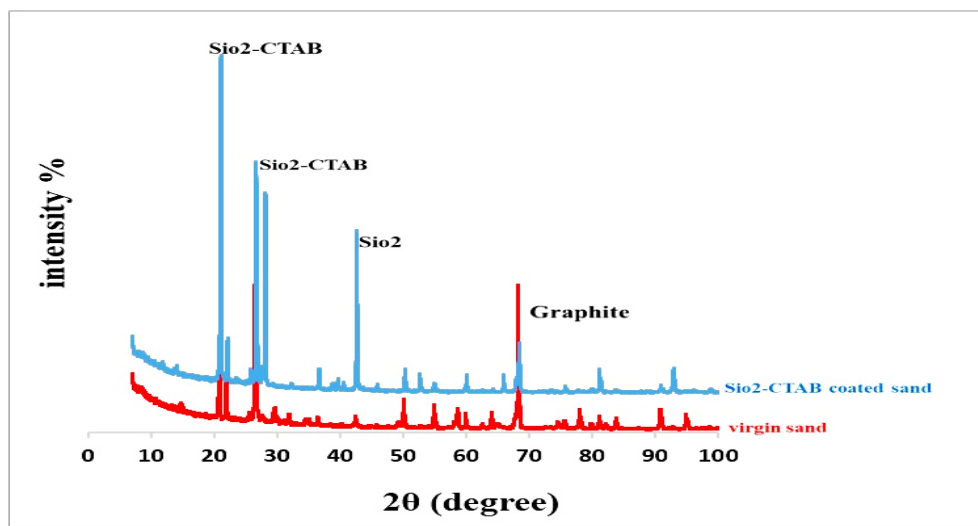


Figure 2. XRD patterns of coated and virgin sand

FTIR spectra Figure 3 for the coated sand, before and after Pb loading, revealed key functional groups involved in metal binding. A broad O–H stretching peak appeared at  $\sim 3438\text{ cm}^{-1}$ , indicating surface hydroxyl groups. Strong Si–O–Si and Si–O vibrations were observed between  $800\text{--}1137\text{ cm}^{-1}$ , confirming the presence of nanosilica. Peaks near  $2925$  and  $2852\text{ cm}^{-1}$  correspond to C–H stretching, associated with CTAB. Additional bands around  $1600\text{ cm}^{-1}$  were attributed to C=C vibrations, while a C–O band was detected near  $1263\text{ cm}^{-1}$ . Notably, post-adsorption spectra exhibited slight shifts in key peaks and intensity variations, suggesting active interaction between  $\text{Pb}^{2+}$  ions and surface groups via ion exchange, hydrogen bonding, and electrostatic forces (Kalam et al., 2021; Khitous et al., 2016). These spectral changes confirm the functional role of hydroxyl, silicate, and organic groups in lead removal.

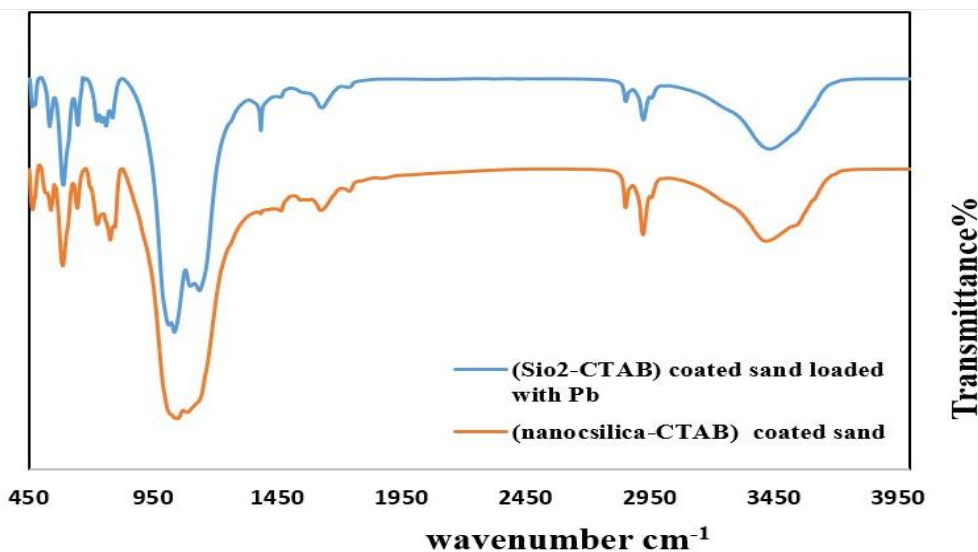


Figure 3. FTIR spectra before and after Pb adsorption

FESEM images (Figure 4) illustrate morphological differences between raw sand, coated sand, and Pb-loaded composite. Virgin sand showed a rough, irregular texture, while coating introduced heterogeneous layers that increased surface roughness and potential active sites. After Pb adsorption, notable morphological changes were observed, suggesting strong surface interaction. BET analysis confirmed a surface area increase from  $3.40\text{ m}^2/\text{g}$  (raw) to  $4.10\text{ m}^2/\text{g}$  after coating.

EDS spectra (Figure 5) revealed elemental shifts post-modification. Silicon and carbon content rose from 19.0% and 7.4% in virgin sand to 40.0% and 13.6%, confirming successful nanosilica/CTAB deposition. After lead uptake, Pb signals appeared at 39.1%, while oxygen and silica decreased, indicating active ion exchange and surface complexation.

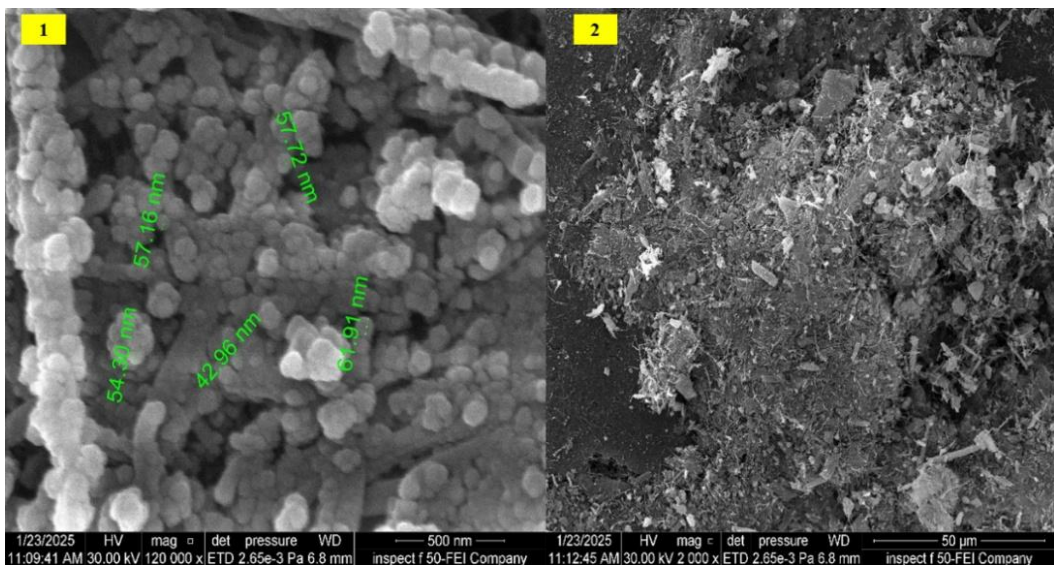


Figure 4a. FESEM image of virgin sand surface

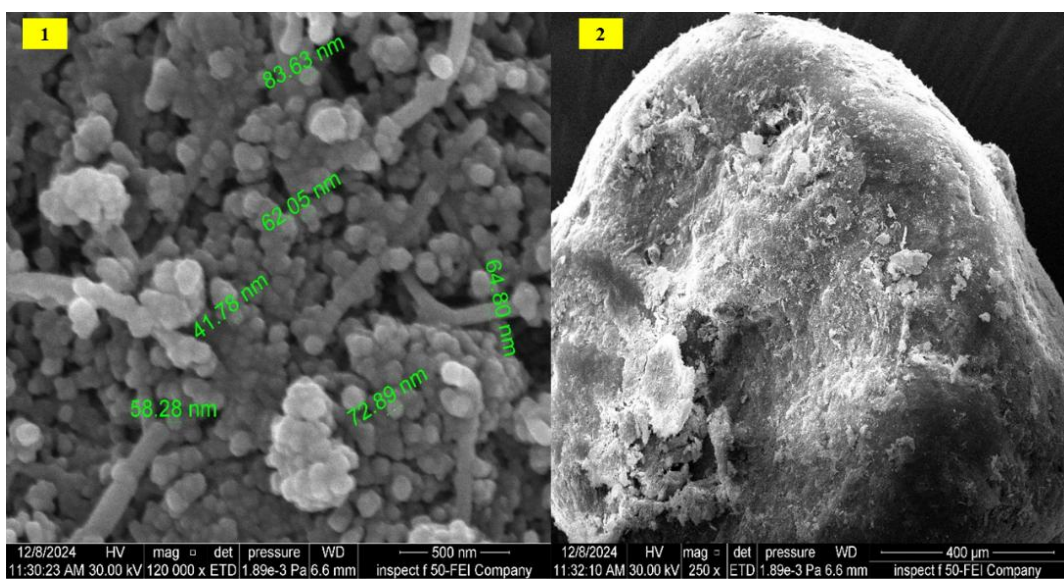


Figure 4b. FESEM image of coated sand surface

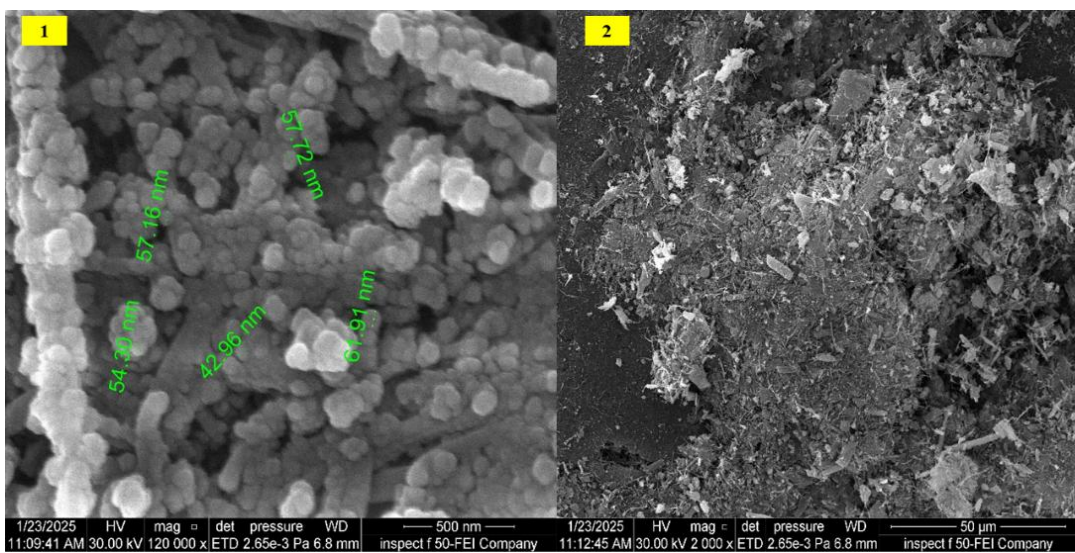


Figure 4c. FESEM image after Pb adsorption

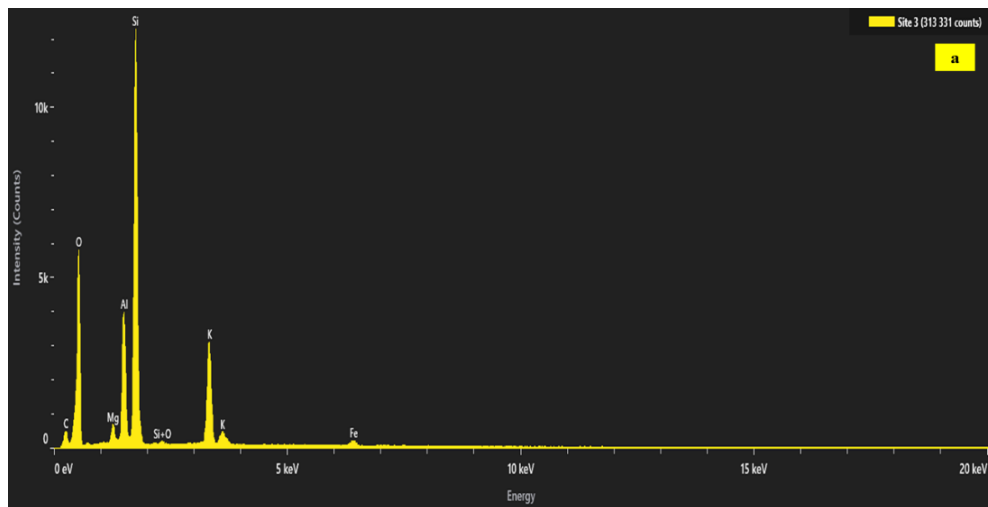


Figure 5a. EDS spectrum of virgin sand

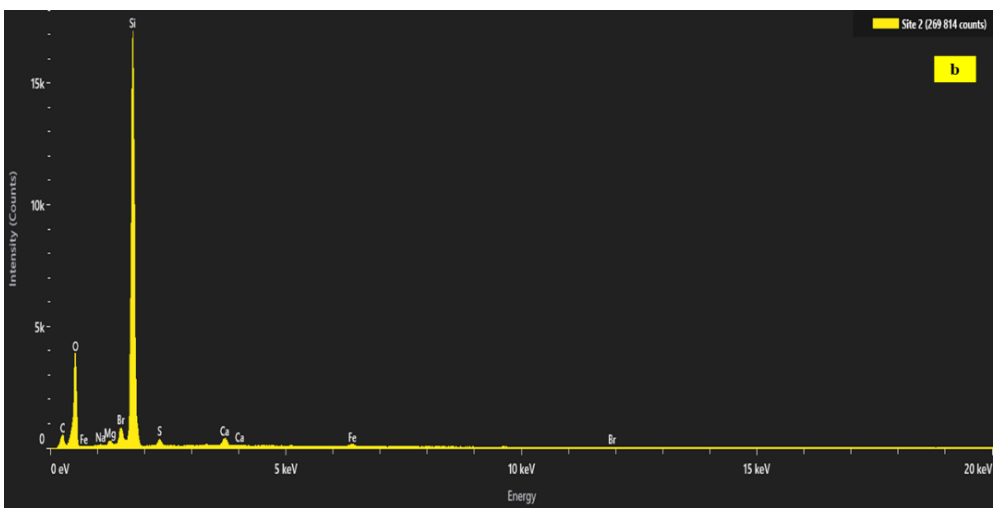


Figure 5b. EDS spectrum of coated sand

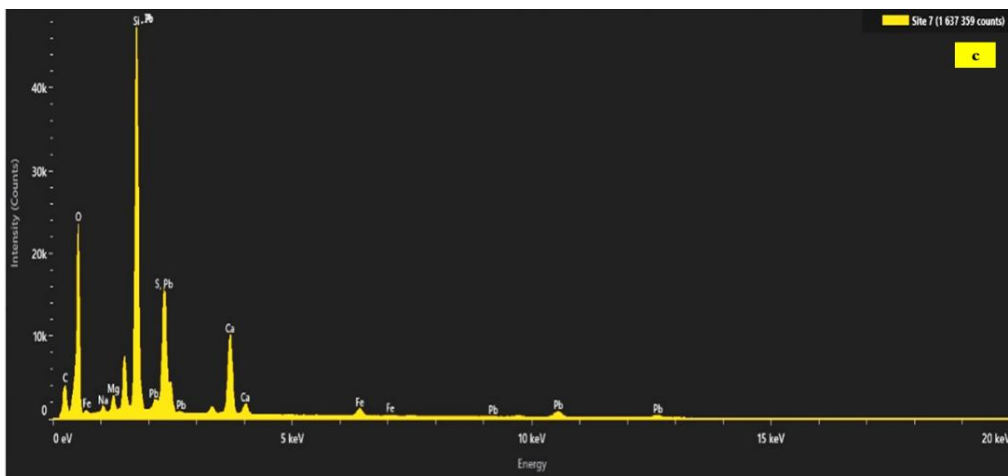


Figure 5c. EDS spectrum after Pb adsorption

Despite the modest increase in surface area from 2.22 to 3.51  $\text{m}^2/\text{g}$  (Figure 6), the coated sand exhibited a significant enhancement in  $\text{Pb}^{2+}$  removal. BET analysis confirmed a rise in total pore volume and average pore diameter, from 0.0083 to 0.0120  $\text{cm}^3/\text{g}$  and from 9.77 to 11.70 nm, respectively. These improvements—though moderate—suggest better accessibility and dispersion of active sites due to the CTAB–nanosilica coating, which facilitated stronger metal–surface interactions and more effective ion exchange.

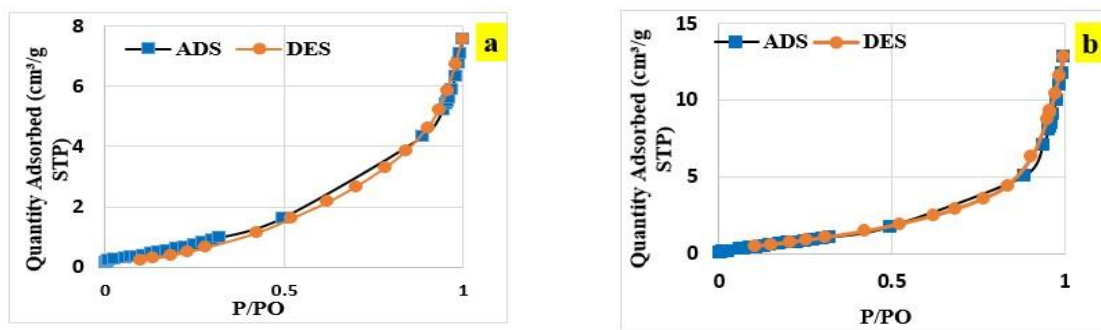


Figure 6. BET isotherms of virgin and coated sand

### Effect of Water Flowrate

The effect of water flow rate on the sorption of Pb ions onto a coated sand barrier was investigated using two flow rate values: 5 and 15 mL/minute. The plots in Figure 7 were created with Cin at a concentration of 50 mg/L, the given flow rates, and a height of 50 cm. The increased discharge may be connected with a shorter breakthrough time and an elevation in the plot's slope. Consequently, the "retention time" is insufficient, resulting in the influent metal molecules fleeing prior to reaching the equilibrium state.(Ko et al., 2000). Furthermore, increasing flow velocity may reduce the adhesion between solute and solid particles, resulting in a large decrease in removal percentage (Kundu & Gupta, 2007). As a result, the solute's retention period in the packed bed was insufficient to achieve sorption equilibrium at the desired discharge. As a result, the solute will escape the bed before it has a chance to bind to the coated sand's active sites, resulting in premature occurrence. Changing the flow rate from 5 to 15 mL/min for Pb Cin at a concentration of 50 mg/L will significantly reduce the "breakthrough time" from 186 to 72 hours.

An increase in discharge will speed up the emergence of the chemical front, shorten the "breakthrough time," and make the "breakthrough curves" steeper, because the chemical will depart the bed before reaching equilibrium. A significant discharge can potentially desorb many linked molecules from the sorbent surface if the connections are weak and reversible. As a result, the metal content in the effluent rapidly increases, accelerating the "breakthrough time," which is facilitated by a low flow rate. The selected flow rates (5 and 15 mL/min) were chosen to ensure laminar flow conditions (Reynolds number < 10), which better simulate natural groundwater movement in subsurface environments.

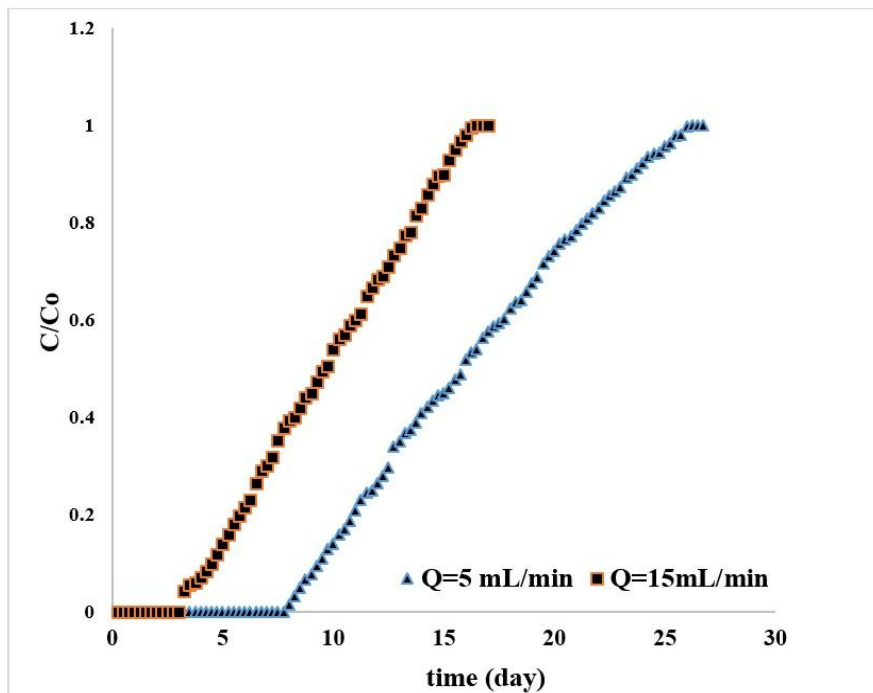


Figure 7. Breakthrough curves at two flow rates

Additionally, while the current study did not include pH variation, the influence of pH on the adsorption performance of the coated media was previously investigated in a separate study using the same CTAB–nanosilica-modified sand. That work demonstrated optimal lead removal within the pH of 5, which aligns with typical groundwater conditions (pH 5–8.5). Therefore, this study focused on evaluating dynamic adsorption behavior under controlled flow conditions.

The increased flow rate may desorb part of the bound solute molecules due to reversible and loose interactions with the sorbent surface. As a result, the metal concentration in the effluent rapidly increases, resulting in a shorter breakthrough time for metal removal in the packed bed due to its increased adsorption capacity. The observed findings are consistent with previous study (Liao et al., 2013; Marzbali & Esmaili, 2017).

### Modelling of Breakthrough Curves

Metal ions breakthrough curves measured along the coated sand bed at different discharges and inlet concentration (50 mg/l) for depth of 50 cm are formulated by number of familiar models mentioned in the paragraph “Description of breakthrough curves data” as plotted in Figures 8a and 8b. The models are represented by "Bohart-Adams, Thomas-BDST, Belter-Cussler-Hu, Yan and Clark" expressions which simulated the trends of curves at 50 cm. The selected models were chosen to represent a broad spectrum of adsorption behaviors, covering kinetic, mass transfer, and empirical response frameworks commonly applied in fixed-bed systems. While alternative models like Yoon–Nelson or Wolborska offer value, the five employed here provide sufficient descriptive and comparative power for the study’s objectives.

The breakthrough curves presented in this study were generated from continuous flow experiments conducted over 27 days, with samples collected every 6 hours for each flow condition (5 and 15 mL/min). While this provides detailed temporal resolution, the study did not include replicate runs for each experimental condition. Therefore, standard deviation and error bars could not be computed for individual time points.

The "solver option in Microsoft Excel 2016 for nonlinear regression" was applied to determine the fit between these models and experimental measurements. The outputs of the fitting process, summarized in Tables 1 and 2, revealed a high degree of correlation between experimental and simulated breakthrough curves, particularly for the Bohart-Adams, Thomas-BDST, Belter-Cussler-Hu, and Clark models ( $R^2 > 0.99$ ; SSE < 0.26). This strong fit indicates a consistent and predictable adsorption process dominated by pseudo-second-order kinetics and film diffusion control, as inferred from the Thomas and Belter-Cussler-Hu models.

The Clark model, which integrates Freundlich isotherms with mass-transfer resistance, provided the best statistical match ( $R^2 = 0.994$  at 5 mL/min), implying that multilayer adsorption and non-uniform energy distribution are likely mechanisms. Such behavior aligns with previous studies on CTAB-modified surfaces, where surfactant molecules introduce hydrophobic regions enhancing  $Pb^{2+}$  attraction (de Franco et al., 2017; Nguyen et al., 2015). Furthermore, the slightly reduced fit of the Yan model at both flowrates ( $R^2 < 0.93$ ) may stem from its limited ability to simulate rapid transitions at the breakthrough front, especially under high influent velocities. This suggests the dominance of surface affinity and pore diffusion rather than abrupt sorption-deactivation dynamics.

Compared to conventional PRB media such as biochar and zeolites, the CTAB–nanosilica-coated sand developed in this study exhibits enhanced adsorption performance under dynamic flow conditions. Biochar, while cost-effective and environmentally benign, often suffers from surface heterogeneity and limited breakthrough resistance in continuous systems, which reduces its overall effectiveness (Siggins, 2025). Zeolites, although widely used for ion-exchange applications, tend to demonstrate slower adsorption kinetics and lower capacity in column configurations due to diffusion limitations (Rocha & Zuquette, 2020). The coated sand presented here offers a balance of surface reactivity and hydraulic conductivity, making it a promising candidate for scalable and efficient PRB implementations.

Upon examining Figure and 8, it is evident that error bars are not presented. This is because replicate runs were not performed during the column experiments due to time and material constraints. Consequently, standard deviations could not be calculated. Future studies are encouraged to incorporate triplicate runs for each experimental condition to improve statistical reliability and enable error analysis. While the breakthrough model parameters ( $K_T$ ,  $n$ ,  $q_0$ ) were derived from column data, their physical relevance is supported by separate batch adsorption studies conducted by the authors. These experiments, reported in a parallel manuscript under review, confirmed pseudo-second-order kinetic behavior with strong correlation ( $R^2 > 0.99$ ) and equilibrium reached

within 120 minutes. Thus, the kinetic assumptions of the Thomas and Clark models are consistent with independent kinetic validation.

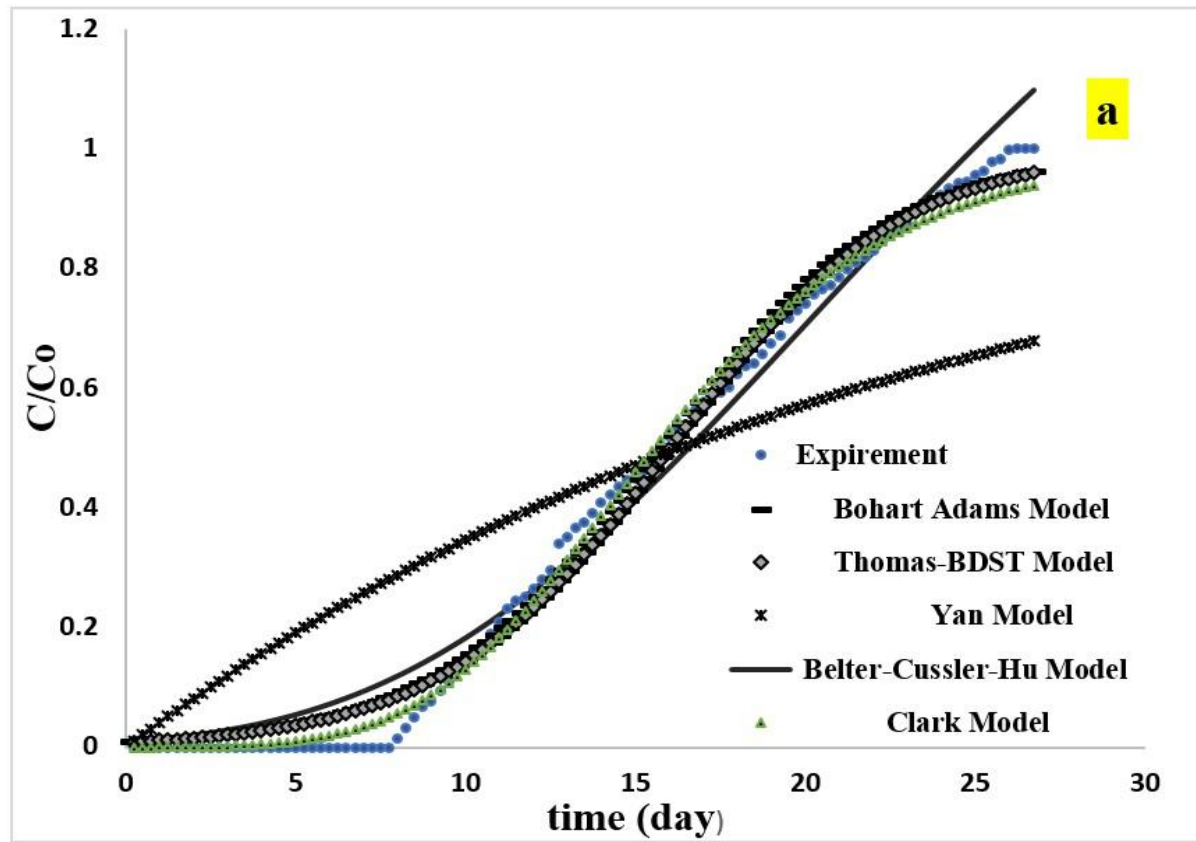


Figure 8a. Breakthrough modeling curve at 5 mL/min flow

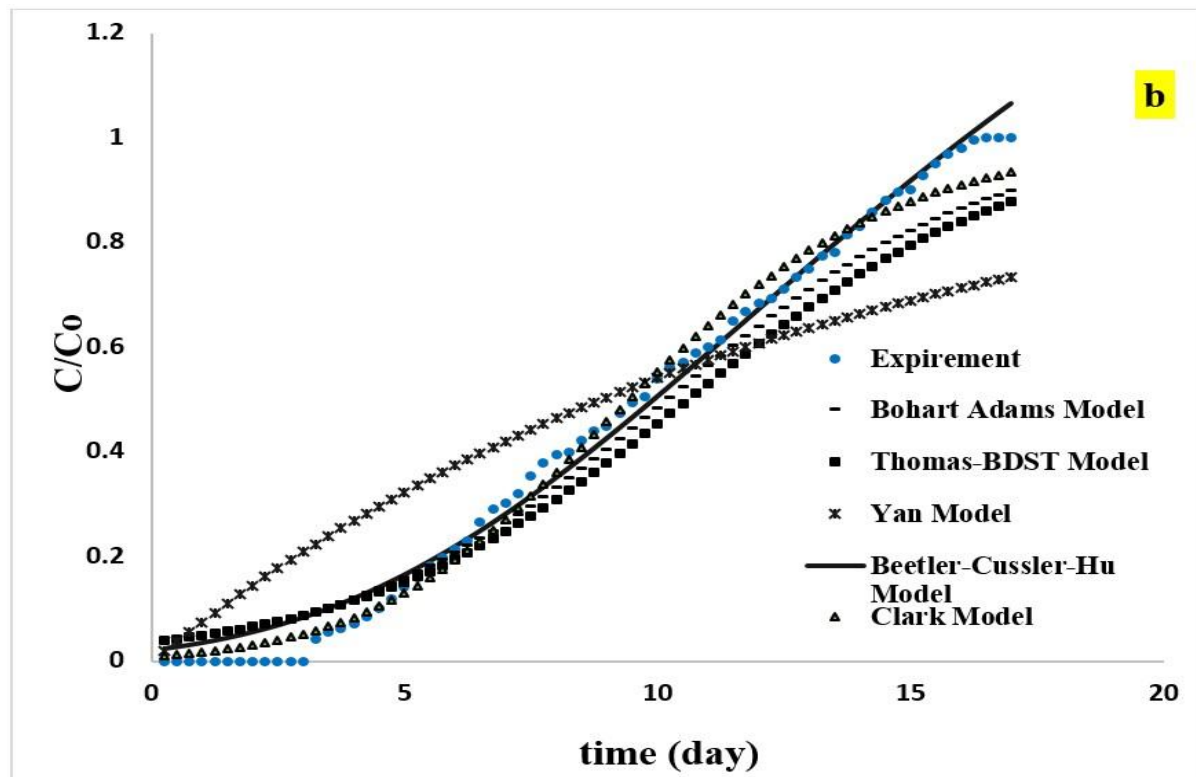


Figure 8b. Breakthrough curve modeling at 15 mL/min flow

Table 1. The fitting parameters of the selected models applied to lead-ion breakthrough curves measured at a 50 cm depth, with an influent concentration of 50 mg/L and a flow rate of 5 mL/min.

Model	Parameter	Cin (mg/L) = 50
Bohart-Adams	KCo	0.9267
	KNoZ/U	4.7376
	R <sup>2</sup>	0.9923
	SSE	0.1239
Thomas-BDST	K <sub>T</sub> Co	0.9256
	K <sub>Tq</sub> M/Q	4.7363
	R <sup>2</sup>	0.9921
	SSE	0.1245
Yan	0.001QC/q <sub>0</sub> M	7.1389
	<i>a</i>	595.9962
	R <sup>2</sup>	0.8957
	SSE	3.8025
Belter-Cussler-Hu	$\sigma$	0.385
	t <sub>0</sub>	24.9591
	R <sup>2</sup>	0.9843
	SSE	0.2509
Clark	A	5.1262
	r	0.2214
	n	1.2181
	R <sup>2</sup>	0.9946
	SSE	0.0801

Table 2. The fitting outputs of the selected models for lead-ion breakthrough curves measured at a 50 cm bed depth, with an influent concentration of 50 mg/L and a flow rate of 15 mL/min.

Model	Parameter	Cin (mg/L) = 50
Bohart-Adams	KCo	0.3200
	KNoZ/U	3.2653
	R <sup>2</sup>	0.9937
	SSE	0.2589
	K <sub>T</sub> Co	0.3200
	K <sub>Tq</sub> M/Q	3.2653
Thomas-BDST	R <sup>2</sup>	0.9924
	SSE	0.4266
	0.001QC/q <sub>0</sub> M	0.000187
	<i>a</i>	780.4153
	R <sup>2</sup>	0.9327
	SSE	1.5862
Belter-Cussler-Hu	$\sigma$	0.4342
	t <sub>0</sub>	16.0821
	R <sup>2</sup>	0.9919
	SSE	0.0760
Clark	A	9.5023
	r	0.3289
	n	1.5113
	R <sup>2</sup>	0.9909
	SSE	0.0792

### Hydraulic Conductivity

The hydraulic conductivities of the coated sand in the column were evaluated at specific intervals using the hydraulic gradient and the cumulative volume of processed water. The results indicated that the hydraulic conductivities were approximately stabilized at  $2.55 \times 10^{-2}$  cm/s during the entire duration of the experimental operation. This behavior may come from the likelihood of no precipitate forming within the packed bed. Thus, the gaps in the packed bed will retain their accessibility for water movement and, subsequently, the transport of solute within the bed. While post-adsorption XRD spectra exhibited slight shifts and intensity changes, the analysis did not conclusively identify crystalline lead compounds (e.g., PbSiO<sub>3</sub>). Further investigation using

comparative XRD with ICDD standards or ICP-MS analysis is recommended to determine if precipitation occurred and assess its potential impact on long-term pore clogging. The suitable conductivities for PRB exceed  $2.1 \times 10^{-2}$  cm/s, as shown in prior research, and this aligns with current data.

#### *Durability and Regeneration Potential of the Coated Barrier*

Although the test duration was limited to 27 days, the coated media demonstrated effective lead removal over extended periods. At the lower flow rate, the material maintained efficiency for nearly 186 hours before nearing saturation. This suggests a potential column lifetime of up to 7.7 days per 50 cm bed under moderate hydraulic loads.

Previous studies have shown that materials modified with CTAB exhibit similar exhaustion times due to surface saturation or gradual loss of active sites (Masood & Abd Ali, 2020). While CTAB enhances adsorption, it may reduce long-term performance by partially blocking pore spaces. Therefore, future work should evaluate regeneration through chemical washing (e.g., dilute acid or surfactant solution) and simulate performance under field conditions using models such as MODFLOW or GMS (Deshmukh, M.; Pathan, 2025; Zhao et al., 2022).

Although this study demonstrated the coated media's potential for sustained lead removal, no regeneration experiments were conducted to evaluate reusability. It is strongly recommended that future studies include desorption tests using mild acids (e.g., HCl) or surfactant rinses to quantify regeneration efficiency across multiple cycles. Additionally, the structural integrity and adsorption performance of the media post-regeneration should be assessed to better understand its practical field applicability and determine the economic feasibility of its long-term use.

## **Conclusion**

This study confirmed the efficacy of a novel reactive medium, comprising sand particles coated with nanosilica and functionalised with cetyltrimethylammonium bromide (CTAB), for lead extraction from contaminated water under continuous flow conditions. The synthesis method produced a material with a uniform coating and excellent hydraulic properties, maintaining a permeability rate of approximately  $2.55 \times 10^{-2}$  cm/s for 27 days. The analysis of breakthrough curves showed that the speed of the flow had a big effect on how well the lead could be removed. The medium worked better for longer when the flow rates were slower. The experimental observations were in close agreement with the Clark and Thomas-BDST models, indicating adsorption behaviour that is consistent with multilayer formation and pseudo-second-order kinetics. These results show that the composite material that was made is a good fit for use in permeable reactive barrier (PRB) systems that are meant to reduce heavy metal pollution.

The results also show how important CTAB is for making particles spread out better, stick together better, and interact with lead ions on the surface. However, the material's effectiveness may not last as long as it should because of problems like pore clogging and saturation of active sites. To address these challenges, subsequent research should examine regeneration techniques utilising mild acid or surfactant rinses, alongside evaluating the media's efficacy in extensive applications via hydrogeological modelling platforms such as MODFLOW or GMS.

In conclusion, the CTAB-functionalized nanosilica-coated sand medium offers a promising, economical, and ecologically sound method for in-situ remediation of lead in groundwater, aiding the advancement of sustainable water purification technologies.

## **Recommendations**

1. Evaluate the feasibility of using the sorbent prepared in this study as a core material for the application of permeable reactive barrier (PRB) technology at the field scale for the remediation of contaminated groundwater.
2. Expand the scope of research to include dynamic flow conditions and pH fluctuations, regeneration for sorbent, alternative PRB configurations, such as the "funnel and gate" system, to monitor the theoretical and experimental migration of metal ions in two- and three-dimensional subsurface media.

## Scientific Ethics Declaration

\* The authors declare that the scientific ethical and legal responsibility of this article published in EPSTEM journal belongs to the authors.

## Conflict of Interest

\* The authors declare that they have no conflicts of interest

## Funding

\* No funding was received for this study.

## Acknowledgements or Notes

\* This article was presented as an oral presentation at the International Conference on Engineering and Advanced Technology (ICEAT) held in Selangor, Malaysia on July 23-24, 2025.

## References

Chu, K. H., Feng, X., Kim, E. Y., & Hung, Y.-T. (2011). Biosorption parameter estimation with genetic algorithm. *Water*, 3(1), 177–195.

Clark, R. M. (1987). Evaluating the cost and performance of field-scale granular activated carbon systems. *Environmental Science & Technology*, 21(6), 573–580.

de Franco, M. A. E., de Carvalho, C. B., Bonetto, M. M., de Pelegrini Soares, R., & Féris, L. A. (2017). Removal of amoxicillin from water by adsorption onto activated carbon in batch process and fixed bed column: Kinetics, isotherms, experimental design and breakthrough curves modelling. *Journal of Cleaner Production*, 161, 947–956.

Deshmukh, M., & Pathan, A. (2025). Advancements and challenges in the use of surfactants and nanoparticles for enhanced oil recovery: Mechanisms, synergies, and field applications. *Environmental Science and Pollution Research*, 1–35.

Kalam, S., Abu-Khamsin, S. A., Kamal, M. S., & Patil, S. (2021). Surfactant adsorption isotherms: A review. *ACS Omega*, 6(48), 32342–32348.

Khitous, M., Salem, Z., & Halliche, D. (2016). Removal of phosphate from industrial wastewater using uncalcined MgAl-NO<sub>3</sub> layered double hydroxide: Batch study and modeling. *Desalination and Water Treatment*, 57(34), 15920–15931.

Ko, D. C. K., Porter, J. F., & McKay, G. (2000). Optimised correlations for the fixed-bed adsorption of metal ions on bone char. *Chemical Engineering Science*, 55(23), 5819–5829.

Kundu, S., & Gupta, A. K. (2007). As (III) removal from aqueous medium in fixed bed using iron oxide-coated cement (IOCC): Experimental and modeling studies. *Chemical Engineering Journal*, 129(1–3), 123–131.

Liao, P., Zhan, Z., Dai, J., Wu, X., Zhang, W., Wang, K., & Yuan, S. (2013). Adsorption of tetracycline and chloramphenicol in aqueous solutions by bamboo charcoal: A batch and fixed-bed column study. *Chemical Engineering Journal*, 228, 496–505.

Liu, C., Sun, Y., Yu, Q., Niu, C., Soomro, S., & Hu, C. (2022). A comprehensive framework model for the trend, period and evaluation of the precipitation enhancement effect: TPEM. *Water Supply*, 22(8), 6558–6575.

Madan, S. S., De, B. S., & Wasewar, K. L. (2019). Adsorption performance of packed bed column for benzylformic acid removal using CaO<sub>2</sub> nanoparticles. *Chemical Data Collections*, 23, 100267.

Marzbali, M. H., & Esmaeli, M. (2017). Fixed bed adsorption of tetracycline on a mesoporous activated carbon: Experimental study and neuro-fuzzy modeling. *Journal of Applied Research and Technology*, 15(5), 454–463.

Masood, Z. B., & Abd Ali, Z. T. (2020). Numerical modeling of two-dimensional simulation of groundwater protection from lead using different sorbents in permeable barriers. *Environmental Engineering Research*, 25(4), 605–613.

Nguyen Xuan Huan, N. X. H., Tran Nam Anh, T. N. A., Nguyen Thi Thuy Hang, N. T. T. H., Dao Thi Tuyet Nhung, D. T. T. N., & Nguyen Van Thanh, N. V. T. (2018). Nanosilica synthesis and application for lead treatment in water. *Journal of Vietnamese Environment*, 9(5), 255-263.

Nguyen, T. A. H., Ngo, H. H., Guo, W. S., Pham, T. Q., Li, F. M., Nguyen, T. V., & Bui, X. T. (2015). Adsorption of phosphate from aqueous solutions and sewage using zirconium loaded okara (ZLO): Fixed-bed column study. *Science of the Total Environment*, 523, 40-49.

Radhika, R., Jayalatha, T., Jacob, S., Rajeev, R., & George, B. K. (2018). Adsorption performance of packed bed column for the removal of perchlorate using modified activated carbon. *Process Safety and Environmental Protection*, 117, 350-362.

Rocha, L. C. C., & Zuquette, L. V. (2020). Evaluation of zeolite as a potential reactive medium in a permeable reactive barrier (PRB): Batch and column studies. *Geosciences*, 10(2), 59.

Salami, B. A., Oyehan, T. A., Gambo, Y., Badmus, S. O., Tanimu, G., Adamu, S., Lateef, S. A., & Saleh, T. A. (2022). Technological trends in nanosilica synthesis and utilization in advanced treatment of water and wastewater. *Environmental Science and Pollution Research*, 29(28), 42560-42600.

Schnase, J. L., & Cunnias, E. L. (Eds.). (1995). *Proceedings from CSCL '95: The First International Conference on Computer Support for Collaborative Learning*. Erlbaum.

Schultz, S. (2005). Calls made to strengthen state energy policies. *The Country Today*, pp. 1A, 2A.

Scruton, R. (1996). The eclipse of listening. *The New Criterion*, 15(30), 5-13.

Siggins, A. (2025). Biochar-based permeable reactive barriers. In *Biochar amendments for environmental remediation* (pp. 213-225). CRC Press.

Wang, B., Xin, S., Jin, D., Zhang, L., Wu, J., & Guo, H. (2024). A new porosity evaluation method based on a statistical methodology for granular material: A case study in construction sand. *Applied Sciences*, 14(16), 7379.

Yaqubi, O., Tai, M. H., Mitra, D., Gerente, C., Neoh, K. G., Wang, C.-H., & Andres, Y. (2021). Adsorptive removal of tetracycline and amoxicillin from aqueous solution by leached carbon black waste and chitosan-carbon composite beads. *Journal of Environmental Chemical Engineering*, 9(1), 104988.

Ye, Y., Wei, Y., Gu, Y., Kang, D., Jiang, W., & Kang, J. (2020). Simultaneous removal of fluoride and phosphate in a continuous fixed-bed column filled with magnesia-pullulan composite. *Journal of Alloys and Compounds*, 838, 155528.

Zhao, L., Wang, X., & Liu, Z. (2022). Research on PRB technology for groundwater remediation. *International Conference on Environmental Pollution and Governance*, 691-696.

---

### Author(s) Information

---

**Hanaf Khalf**

Al-Furat Al-Awsat Technical University

Najaf/Iraq

Contact e-mail: hanan.hussam.1994@gmail.com

**Thulfiqar Al-Husseini**

Al-Qadisiyah University/College of Engineering/ Civil Eng

Diwaniyah/Iraq

**Entessar Hussain**

Al- Qadisiyah University/College of Engineering/ Civil Eng

Diwaniyah/Iraq

---

**To cite this article:**

Khalaf, H., Al-Husseini, T., & Hussain, E. (2025). Lead removal from water using CTAB-enhanced nanosilica-coated sand barrier under continuous flow: Experimental study and breakthrough curve modelling. *The Eurasia Proceedings of Science, Technology, Engineering and Mathematics (EPSTEM)*, 37, 629-642.